

Direct Measurement of the Top Quark Mass

S. Abachi,¹⁴ B. Abbott,²⁸ M. Abolins,²⁵ B. S. Acharya,⁴³ I. Adam,¹² D. L. Adams,³⁷ M. Adams,¹⁷ S. Ahn,¹⁴ H. Aihara,²² G. A. Alves,¹⁰ E. Amidi,²⁹ N. Amos,²⁴ E. W. Anderson,¹⁹ R. Astur,⁴² M. M. Baarmand,⁴² A. Baden,²³ V. Balamurali,³² J. Balderston,¹⁶ B. Baldin,¹⁴ S. Banerjee,⁴³ J. Bantly,⁵ E. Barberis,²² J. F. Bartlett,¹⁴ K. Bazizi,³⁹ A. Belyaev,²⁶ S. B. Beri,³⁴ I. Bertram,³¹ V. A. Bezzubov,³⁵ P. C. Bhat,¹⁴ V. Bhatnagar,³⁴ M. Bhattacharjee,¹³ N. Biswas,³² G. Blazey,³⁰ S. Blessing,¹⁵ P. Bloom,⁷ A. Boehnlein,¹⁴ N. I. Bojko,³⁵ F. Borchering,¹⁴ J. Borders,³⁹ C. Boswell,⁹ A. Brandt,¹⁴ R. Brock,²⁵ A. Bross,¹⁴ D. Buchholz,³¹ V. S. Burtovoi,³⁵ J. M. Butler,³ W. Carvalho,¹⁰ D. Casey,³⁹ H. Castilla-Valdez,¹¹ D. Chakraborty,⁴² S.-M. Chang,²⁹ S. V. Chekulaev,³⁵ L.-P. Chen,²² W. Chen,⁴² S. Choi,⁴¹ S. Chopra,²⁴ B. C. Choudhary,⁹ J. H. Christenson,¹⁴ M. Chung,¹⁷ D. Claes,²⁷ A. R. Clark,²² W. G. Cobau,²³ J. Cochran,⁹ W. E. Cooper,¹⁴ C. Cretsinger,³⁹ D. Cullen-Vidal,⁵ M. A. C. Cummings,¹⁶ D. Cutts,⁵ O. I. Dahl,²² K. Davis,² K. De,⁴⁴ K. Del Signore,²⁴ M. Demarteau,¹⁴ D. Denisov,¹⁴ S. P. Denisov,³⁵ H. T. Diehl,¹⁴ M. Diesburg,¹⁴ G. Di Loreto,²⁵ P. Draper,⁴⁴ J. Drinkard,⁸ Y. Ducros,⁴⁰ L. V. Dudko,²⁶ S. R. Dugad,⁴³ D. Edmunds,²⁵ J. Ellison,⁹ V. D. Elvira,⁴² R. Engelmann,⁴² S. Eno,²³ G. Eppley,³⁷ P. Ermolov,²⁶ O. V. Eroshin,³⁵ V. N. Evdokimov,³⁵ T. Fahland,⁸ M. Fatyga,⁴ M. K. Fatyga,³⁹ J. Featherly,⁴ S. Feher,¹⁴ D. Fein,² T. Ferbel,³⁹ G. Finocchiaro,⁴² H. E. Fisk,¹⁴ Y. Fisysak,⁷ E. Flattum,²⁵ G. E. Forden,² M. Fortner,³⁰ K. C. Frame,²⁵ S. Fuess,¹⁴ E. Gallas,⁴⁴ A. N. Galyaev,³⁵ P. Gattung,⁹ T. L. Geld,²⁵ R. J. Genik, II,²⁵ K. Genser,¹⁴ C. E. Gerber,¹⁴ B. Gibbard,⁴ S. Glenn,⁷ B. Gobbi,³¹ M. Goforth,¹⁵ A. Goldschmidt,²² B. Gómez,¹ G. Gómez,²³ P. I. Goncharov,³⁵ J. L. González Solís,¹¹ H. Gordon,⁴ L. T. Goss,⁴⁵ A. Goussiou,⁴² N. Graf,⁴ P. D. Grannis,⁴² D. R. Green,¹⁴ J. Green,³⁰ H. Greenlee,¹⁴ G. Grim,⁷ S. Grinstein,⁶ N. Grossman,¹⁴ P. Grudberg,²² S. Grünendahl,³⁹ G. Guglielmo,³³ J. A. Guida,² J. M. Guida,⁵ A. Gupta,⁴³ S. N. Gurzhiev,³⁵ P. Gutierrez,³³ Y. E. Gutnikov,³⁵ N. J. Hadley,²³ H. Haggerty,¹⁴ S. Hagopian,¹⁵ V. Hagopian,¹⁵ K. S. Hahn,³⁹ R. E. Hall,⁸ S. Hansen,¹⁴ J. M. Hauptman,¹⁹ D. Hedin,³⁰ A. P. Heinson,⁹ U. Heintz,¹⁴ R. Hernández-Montoya,¹¹ T. Heuring,¹⁵ R. Hirsch,¹⁵ J. D. Hobbs,¹⁴ B. Hoeneisen,^{1,*} J. S. Hoftun,⁵ F. Hsieh,²⁴ Ting Hu,⁴² Tong Hu,¹⁸ T. Huehn,⁹ A. S. Ito,¹⁴ E. James,² J. Jaques,³² S. A. Jerger,²⁵ R. Jesik,¹⁸ J. Z.-Y. Jiang,⁴² T. Joffe-Minor,³¹ K. Johns,² M. Johnson,¹⁴ A. Jonckheere,¹⁴ M. Jones,¹⁶ H. Jöstlein,¹⁴ S. Y. Jun,³¹ C. K. Jung,⁴² S. Kahn,⁴ G. Kalbfleisch,³³ J. S. Kang,²⁰ R. Kehoe,³² M. L. Kelly,³² C. L. Kim,²⁰ S. K. Kim,⁴¹ A. Klatchko,¹⁵ B. Klima,¹⁴ C. Klopfenstein,⁷ V. I. Klyukhin,³⁵ V. I. Kochetkov,³⁵ J. M. Kohli,³⁴ D. Koltick,³⁶ A. V. Kostitskiy,³⁵ J. Kotcher,⁴ A. V. Kotwal,¹² J. Kourlas,²⁸ A. V. Kozelov,³⁵ E. A. Kozlovski,³⁵ J. Krane,²⁷ M. R. Krishnaswamy,⁴³ S. Krzywdzinski,¹⁴ S. Kunori,²³ S. Lami,⁴² H. Lan,^{14,†} R. Lander,⁷ F. Landry,²⁵ G. Landsberg,¹⁴ B. Lauer,¹⁹ A. Leflat,²⁶ H. Li,⁴² J. Li,⁴¹ Q. Z. Li-Demarteau,¹⁴ J. G. R. Lima,³⁸ D. Lincoln,²⁴ S. L. Linn,¹⁵ J. Linnemann,²⁵ R. Lipton,¹⁴ Q. Liu,^{14,†} Y. C. Liu,³¹ F. Lobkowicz,³⁹ S. C. Loken,²² S. Lökös,⁴² L. Lueking,¹⁴ A. L. Lyon,²³ A. K. A. Maciel,¹⁰ R. J. Madaras,²² R. Madden,¹⁵ L. Magaña-Mendoza,¹¹ S. Mani,⁷ H. S. Mao,^{14,†} R. Markeloff,³⁰ L. Markosky,² T. Marshall,¹⁸ M. I. Martin,¹⁴ K. M. Mauritz,¹⁹ B. May,³¹ A. A. Mayorov,³⁵ R. McCarthy,⁴² J. McDonald,¹⁵ T. McKibben,¹⁷ J. McKinley,²⁵ T. McMahon,³³ H. L. Melanson,¹⁴ M. Merkin,²⁶ K. W. Merritt,¹⁴ H. Miettinen,³⁷ A. Mincer,²⁸ J. M. de Miranda,¹⁰ C. S. Mishra,¹⁴ N. Mokhov,¹⁴ N. K. Mondal,⁴³ H. E. Montgomery,¹⁴ P. Mooney,¹ H. da Motta,¹⁰ C. Murphy,¹⁷ F. Nang,² M. Narain,¹⁴ V. S. Narasimham,⁴³ A. Narayanan,² H. A. Neal,²⁴ J. P. Negret,¹ P. Nemethy,²⁸ D. Nešić,⁵ M. Nicola,¹⁰ D. Norman,⁴⁵ L. Oesch,²⁴ V. Oguri,³⁸ E. Oltman,²² N. Oshima,¹⁴ D. Owen,²⁵ P. Padley,³⁷ M. Pang,¹⁹ A. Para,¹⁴ Y. M. Park,²¹ R. Partridge,⁵ N. Parua,⁴³ M. Paterno,³⁹ J. Perkins,⁴⁴ M. Peters,¹⁶ R. Piegaia,⁶ H. Piekarczyk,¹⁵ Y. Pischalnikov,³⁶ V. M. Podstavkov,³⁵ B. G. Pope,²⁵ H. B. Prosper,¹⁵ S. Protopopescu,⁴ D. Pušeljčić,²² J. Qian,²⁴ P. Z. Quintas,¹⁴ R. Raja,¹⁴ S. Rajagopalan,⁴ O. Ramirez,¹⁷ P. A. Rapidis,¹⁴ L. Rasmussen,⁴² S. Reucroft,²⁹ M. Rijssenbeek,⁴² T. Rockwell,²⁵ N. A. Roe,²² P. Rubinov,³¹ R. Ruchti,³² J. Rutherford,² A. Sánchez-Hernández,¹¹ A. Santoro,¹⁰ L. Sawyer,⁴⁴ R. D. Schamberger,⁴² H. Schellman,³¹ J. Sculli,²⁸ E. Shabalina,²⁶ C. Shaffer,¹⁵ H. C. Shankar,⁴³ R. K. Shivpuri,¹³ M. Shupe,² H. Singh,⁹ J. B. Singh,³⁴ V. Sirotenko,³⁰ W. Smart,¹⁴ A. Smith,² R. P. Smith,¹⁴ R. Snihur,³¹ G. R. Snow,²⁷ J. Snow,³³ S. Snyder,⁴ J. Solomon,¹⁷ P. M. Sood,³⁴ M. Sosebee,⁴⁴ N. Sotnikova,²⁶ M. Souza,¹⁰ A. L. Spadafora,²² R. W. Stephens,⁴⁴ M. L. Stevenson,²² D. Stewart,²⁴ D. A. Stoianova,³⁵ D. Stoker,⁸ M. Strauss,³³ K. Streets,²⁸ M. Strovink,²² A. Sznajder,¹⁰ P. Tamburello,²³ J. Tarazi,⁸ M. Tartaglia,¹⁴ T. L. T. Thomas,³¹ J. Thompson,²³ T. G. Trippe,²² P. M. Tuts,¹² N. Varelas,²⁵ E. W. Varnes,²² D. Vitoe,² A. A. Volkov,³⁵ A. P. Vorobiev,³⁵ H. D. Wahl,¹⁵ G. Wang,¹⁵ J. Warchol,³² G. Watts,⁵ M. Wayne,³² H. Weerts,²⁵ A. White,⁴⁴ J. T. White,⁴⁵ J. A. Wightman,¹⁹ S. Willis,³⁰ S. J. Wimpenny,⁹ J. V. D. Wirjawan,⁴⁵ J. Womersley,¹⁴ E. Won,³⁹ D. R. Wood,²⁹ H. Xu,⁵ R. Yamada,¹⁴ P. Yamin,⁴ C. Yanagisawa,⁴² J. Yang,²⁸ T. Yasuda,²⁹

P. Yepes,³⁷ C. Yoshikawa,¹⁶ S. Youssef,¹⁵ J. Yu,¹⁴ Y. Yu,⁴¹ Q. Zhu,²⁸ Z. H. Zhu,³⁹ D. Zieminska,¹⁸ A. Zieminski,¹⁸
E. G. Zverev,²⁶ and A. Zylberstejn⁴⁰

(D0 Collaboration)

- ¹Universidad de los Andes, Bogotá, Colombia
²University of Arizona, Tucson, Arizona 85721
³Boston University, Boston, Massachusetts 02215
⁴Brookhaven National Laboratory, Upton, New York 11973
⁵Brown University, Providence, Rhode Island 02912
⁶Universidad de Buenos Aires, Buenos Aires, Argentina
⁷University of California, Davis, California 95616
⁸University of California, Irvine, California 92697
⁹University of California, Riverside, California 92521
¹⁰LAFEX, Centro Brasileiro de Pesquisas Físicas, Rio de Janeiro, Brazil
¹¹CINVESTAV, Mexico City, Mexico
¹²Columbia University, New York, New York 10027
¹³Delhi University, Delhi, India 110007
¹⁴Fermi National Accelerator Laboratory, Batavia, Illinois 60510
¹⁵Florida State University, Tallahassee, Florida 32306
¹⁶University of Hawaii, Honolulu, Hawaii 96822
¹⁷University of Illinois at Chicago, Chicago, Illinois 60607
¹⁸Indiana University, Bloomington, Indiana 47405
¹⁹Iowa State University, Ames, Iowa 50011
²⁰Korea University, Seoul, Korea
²¹Kyungshung University, Pusan, Korea
²²Lawrence Berkeley National Laboratory and University of California, Berkeley, Californian 94720
²³University of Maryland, College Park, Maryland 20742
²⁴University of Michigan, Ann Arbor, Michigan 48109
²⁵Michigan State University, East Lansing, Michigan 48824
²⁶Moscow State University, Moscow, Russia
²⁷University of Nebraska, Lincoln, Nebraska 68588
²⁸New York University, New York, New York 10003
²⁹Northeastern University, Boston, Massachusetts 02115
³⁰Northern Illinois University, DeKalb, Illinois 60115
³¹Northwestern University, Evanston, Illinois 60208
³²University of Notre Dame, Notre Dame, Indiana 46556
³³University of Oklahoma, Norman, Oklahoma 73019
³⁴University of Panjab, Chandigarh 16-00-14, India
³⁵Institute for Higher Energy Physics, 142-284 Protvino, Russia
³⁶Purdue University, West Lafayette, Indiana 47907
³⁷Rice University, Houston, Texas 77005
³⁸Universidade Estadual do Rio de Janeiro, Brazil
³⁹University of Rochester, Rochester, New York 14627
⁴⁰CEA, DAPNIA/Service de Physique des Particules, CE-SACLAY, Gif-sur-Yvette, France
⁴¹Seoul National University, Seoul, Korea
⁴²State University of New York, Stony Brook, New York 11794
⁴³Tata Institute of Fundamental Research, Colaba Mumbai 400005, India
⁴⁴University of Texas, Arlington, Texas 76019
⁴⁵Texas A&M University, College Station, Texas 77843

(Received 11 March 1997)

We measure the top quark mass m_t using $t\bar{t}$ pairs produced in the D0 detector by $\sqrt{s} = 1.8$ TeV $p\bar{p}$ collisions in a 125 pb^{-1} exposure at the Fermilab Tevatron. We make a two constraint fit to m_t in $t\bar{t} \rightarrow bW^+\bar{b}W^-$ final states with one W decaying to $q\bar{q}$ and the other to $e\nu$ or $\mu\nu$. Events are binned in fit mass versus a measure of probability for events to be signal rather than background. Likelihood fits to the data yield $m_t = 173.3 \pm 5.6(\text{stat}) \pm 6.2(\text{syst}) \text{ GeV}/c^2$. [S0031-9007(97)03830-1]

PACS numbers: 14.65.Ha, 13.85.Ni, 13.85.Qk

The top quark has a large mass m_t that can be determined to greater fractional precision than is possible for the lighter quarks, which decay after they form hadrons. Since m_t is large, it controls the strength

of quark-loop corrections to tree-level relations among electroweak parameters. If these parameters and m_t are measured precisely, the standard model Higgs boson mass can be constrained.

Direct measurements of m_t have been published as part of the initial observations [1] of $t\bar{t}$ production in $\sqrt{s} = 1.8$ TeV $p\bar{p}$ collisions. At present, the best accuracy in m_t is achieved for lepton + jets ($\ell + \text{jets}$) final states in which one W boson (from $t \rightarrow bW$) decays to $e\nu$ or $\mu\nu$ and the other W decays to a $q\bar{q}$ pair that forms jets. We report a measurement of m_t in the $\ell + \text{jets}$ channel using the $\approx 125 \text{ pb}^{-1}$ exposure of the D0 detector during the 1992–1996 Fermilab Tevatron runs. Since Ref. [1] appeared, our data sample has doubled, and for a fixed sample size our error on m_t has halved.

The D0 detector and our basic methods for triggering, reconstructing events, and identifying particles are described elsewhere [2]. Recent advances include enhanced triggering and reconstruction efficiency for $\mu + \text{jets}$ events, due, in part, to better use of calorimeter data. As a signature of $W \rightarrow \ell\nu$, we require missing energy transverse to the beam (\cancel{E}_T) > 20 GeV and one isolated e or μ (ℓ) with $E_T^\ell > 20$ GeV and pseudorapidity $|\eta_\ell| < 2$ or $|\eta_\mu| < 1.7$. We also demand $\cancel{E}_T^{\text{cal}} > 25$ (20) GeV for $e + \text{jets}$ ($\mu + \text{jets}$) events, where $\cancel{E}_T^{\text{cal}}$ is \cancel{E}_T measured only in the calorimeter. As signatures of the $q\bar{q}$ from W decay and the b and \bar{b} from t and \bar{t} decay, we require ≥ 4 jets reconstructed with cones of half-angle $\Delta\mathcal{R} \equiv (\Delta\phi^2 + \Delta\eta^2)^{1/2} = 0.5$, having $E_T > 15$ GeV and $|\eta| < 2$.

Within $\Delta\mathcal{R} = 0.5$ of a jet axis, additional muons (μ tags) satisfying $p_T^\mu > 4$ GeV/ c and $|\eta_\mu| < 1.7$ arise mainly from b and c quark semileptonic decay. These occur in $\approx 20\%$ of $t\bar{t}$ events but only $\approx 2\%$ of background events [2]. In untagged events, to suppress background we require $E_T^L \equiv |E_T^\ell| + |\cancel{E}_T| > 60$ GeV and $|\eta_W| < 2$ for the $W \rightarrow \ell\nu$, using the smaller of the two solutions for $|\eta_W|$. The latter cut, exhibited in Fig. 1(a), reduces the difference in η_W distributions between data and Monte Carlo (MC) simulated background. We use the HERWIG MC [3] to simulate top signal and the VECBOS MC [4] (with HERWIG fragmentation of partons into jets) to simulate (but not to normalize) the dominant $W + \text{multijet}$ background. The $\approx 20\%$ of background events from non- W sources are modeled by multijet data that barely fail the lepton identification criteria.

To each event passing the above cuts [5], we make a two constraint (2C) kinematic fit [6] to the $t\bar{t} \rightarrow \ell + \text{jets}$ hypothesis by minimizing a $\chi^2 = (\mathbf{v} - \mathbf{v}^*)^T G (\mathbf{v} - \mathbf{v}^*)$, where $\mathbf{v}(\mathbf{v}^*)$ is the vector of measured (fit) variables and G^{-1} is its error matrix. Both reconstructed W masses are constrained to equal the W pole mass, and the same fit mass m_{fit} is assigned to both the t and \bar{t} quarks. If the event contains > 4 accepted jets, only the four jets with highest E_T are used. In $\approx 50\%$ of MC top events, these jets correspond to the $b, \bar{b}, q,$ and \bar{q} . With (without) a μ tag in the event, there are 6 (12) possible fit assignments of these jets to the quarks, each having two solutions to the ν longitudinal momentum p_z^ν . We use m_{fit} only from the permutation with lowest χ^2 , the correct choice for $\approx 20\%$ of MC top events. Because of the ambiguities, m_{fit}

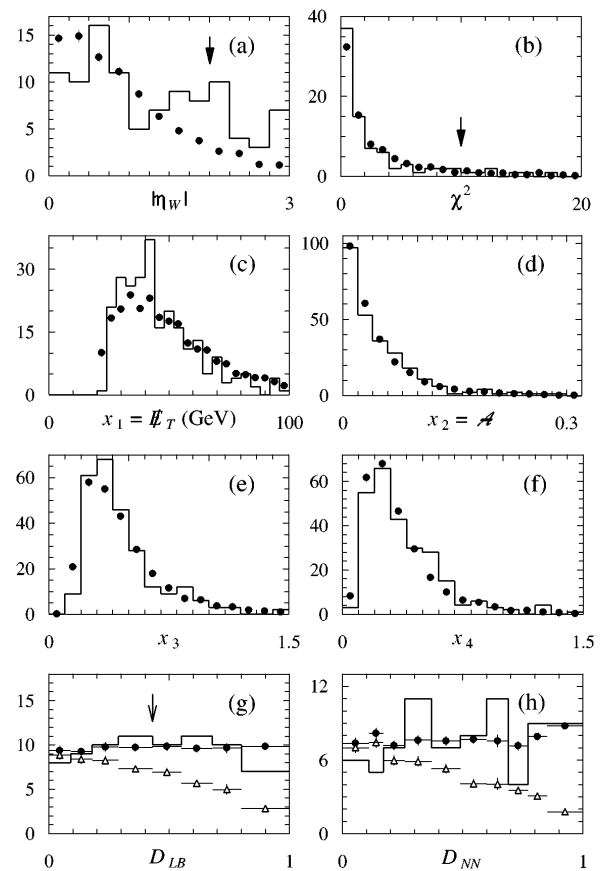


FIG. 1. Events per bin vs event selection variables defined in the text, plotted for (a)–(b), (g)–(h) top quark mass analysis samples, and (c)–(f) $W + 3$ jet control samples. Histograms are data, filled circles are expected top + background mixture, and open triangles are expected background only. Solid arrows in (a)–(b) show cuts applied to all events; the open arrow in (g) illustrates the LB cut. The nonuniform bin widths in (g)–(h) are chosen to yield uniform bin populations.

is not the same as m_t , though they are strongly correlated. Our best estimate of m_t is obtained from the best match between MC samples and the data.

From the 90-event distribution shown in Fig. 1(b) we select 77 events with a 2C fit satisfying $\chi^2 < 10$. Of these, five are μ tagged and $\approx 65\%$ are background. Further separation of signal and background events is based on four kinematic variables $\mathbf{x} \equiv \{x_1, x_2, x_3, x_4\}$ chosen to have small correlation with m_{fit} . On average, all are larger for MC top events than for background events, selected to have the same $\langle m_{\text{fit}} \rangle$ as the top events [7]. The simpler variables are $x_1 \equiv \cancel{E}_T$ and $x_2 = \mathcal{A}$, where aplanarity \mathcal{A} is $\frac{3}{2} \times$ the least eigenvalue of the normalized laboratory momentum tensor of the jets and the W boson. The third variable $x_3 \equiv H_{T2}/H_z$ measures the event's centrality, where H_z is the sum of $|p_z|$ of ℓ, ν , and the jets and H_{T2} is the sum of all jet $|E_T|$ except the highest. Finally, $x_4 \equiv \Delta\mathcal{R}_{jj}^{\text{min}} E_T^{\text{min}} / E_T^L$ measures the extent to which jets are clustered together, where $\Delta\mathcal{R}_{jj}^{\text{min}}$ is the minimum $\Delta\mathcal{R}$ of the six pairs of four jets and E_T^{min} is the smaller jet E_T from the minimum $\Delta\mathcal{R}$ pair. As

shown for the background dominated $W + 3$ jet sample in Figs. 1(c)–1(f), x_1 – x_4 are reasonably well modeled by MC; this is true also for the $W + 2$ jet and top mass samples (not shown).

We bin events in a two-dimensional array with abscissa m_{fit} and ordinate $D(\mathbf{x})$, where D is a multivariate discriminant. To show that our results are robust, we use two methods for which the definition of D , the granularity with which it is binned, and the additional requirements are different. In our “low bias” (LB) method, we first parametrize $\mathcal{L}_i(x_i) \equiv s_i(x_i)/b_i(x_i)$, where s_i and b_i are the top signal and background densities in each variable, integrating over the others. We form the log likelihood $\ln \mathcal{L} = \sum_i \omega_i \ln \mathcal{L}_i$, where the weights ω_i are adjusted slightly away from unity to nullify the average correlation (“bias”) of \mathcal{L} with m_{fit} , and for each event we set $D_{\text{LB}} = \mathcal{L}/(1 + \mathcal{L})$. Finally, we divide the ordinate coarsely into signal- and background-rich bins according to whether the LB cut is passed. This cut is satisfied if a μ tag exists; otherwise it is not satisfied if $D_{\text{LB}} < 0.43$ [Fig. 1(g)] or if $H_{T2} < 90$ GeV.

Our neural network (NN) method is sensitive to the correlations among the x_i as well as to their individual densities. We use a three layer feed-forward NN with four input nodes fed by \mathbf{x} , five hidden nodes, and one output node, trained on samples of top signal [background] with density $s(\mathbf{x})$ [$b(\mathbf{x})$] [8]. For a given event, the network output D_{NN} approximates the ratio $s(\mathbf{x})/[s(\mathbf{x}) + b(\mathbf{x})]$. We divide the ordinate finely into ten bins in D_{NN} , independent of H_{T2} or μ tagging. Figures 1(g) and 1(h) show that D_{LB} and D_{NN} are distributed as predicted and provide comparable discrimination, as we expect when the ω_i are close to unity and the \mathcal{L}_i are not strongly correlated. Figure 2 exhibits the arrays for the NN method. Little correlation between D_{NN} and m_{fit} is evident in the expected signal or background distributions, which are distinct; the data clearly reveal contributions from both sources. Figure 3 shows the distributions of m_{fit} for data (a) passing and (b) failing the LB cut.

To each m_t for which we have generated MC, we assign a likelihood L which assumes that all samples obey Poisson statistics. Bayesian integration [9] over possible true signal and background populations in each bin yields

$$L(m_t, n_s, n_b) = \prod_{i=1}^M \sum_{j=0}^{n_i} \binom{n_{si} + j}{j} \binom{n_{bi} + k}{k} \\ \times p_s^j (1 + p_s)^{-n_{si} - j - 1} \\ \times p_b^k (1 + p_b)^{-n_{bi} - k - 1},$$

where n_s (n_b) is the expected number of signal (background) events in the data; n_i , n_{si} , and n_{bi} are the actual number of data, MC signal, and MC background events in bin i ; $k \equiv n_i - j$; $p_{s,b} \equiv n_{s,b}/(M + \sum_i n_{si,bi})$; and $M = 40$ (200) bins for the LB (NN) methods. Maximizing L for each m_t gives the best estimates $n_s^*(m_t)$ and $n_b^*(m_t)$ for n_s and n_b . Figure 3(c) displays

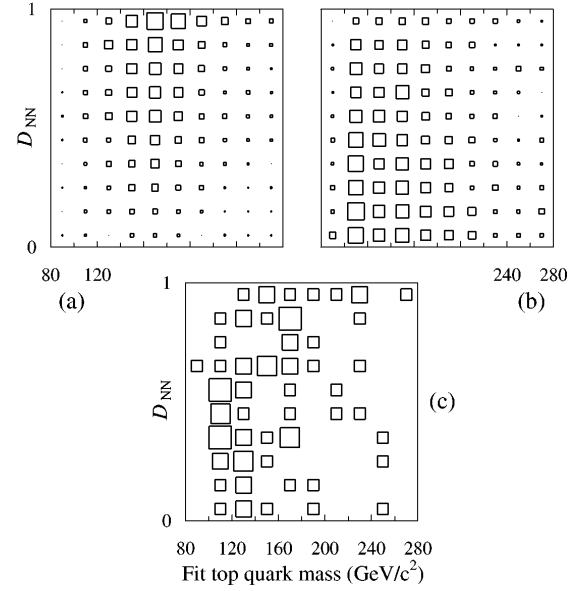


FIG. 2. Events per bin (\propto areas of boxes) vs D_{NN} (ordinate) and m_{fit} (abscissa) for (a) expected 172 GeV/c^2 top signal, (b) expected background, and (c) data. D_{NN} is binned as in Fig. 1(h).

$\ln L(m_t, n_s^*(m_t), n_b^*(m_t))$ vs m_t , where the curves determine the best fit m_t and its statistical error σ_m .

Table I presents the fit results, which are consistent with Ref. [1] and with recent reports [10]. The LB and NN

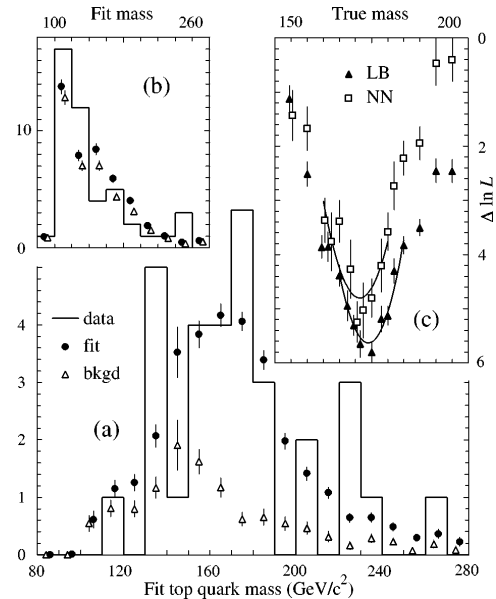


FIG. 3. (a), (b) Events per bin vs m_{fit} for events (a) passing or (b) failing the LB cut. Histograms are data, filled circles are the predicted mixture of top and background, and open triangles are predicted background only. The circles and triangles are the average of the LB and NN fit predictions, which differ by $< 10\%$. (c) Log of arbitrarily normalized likelihood L vs true top quark mass m_t for the LB (filled triangles) and NN (open squares) fits, with errors due to finite top MC statistics. The curves are quadratic fits to the lowest point and its eight nearest neighbors. In MC studies, 7% (27%) of simulated experiments yield a smaller LB (NN) maximum likelihood.

TABLE I. Results of fits to data and MC events. Fits to data yield values and errors σ_{stat} for m_t , n_s , and n_b (described in the text). Systematic errors are combined in quadrature. The resulting m_t and its statistical error σ_m are the combined LB and NN values. Fits to MC use ensembles of 10 000 simulated experiments composed of top + background, with m_t , $\langle n_s \rangle$, and $\langle n_b \rangle$ as listed. They yield a mean result $\langle m_t \rangle$, a mean statistical error $\langle \sigma_m \rangle$, and a range $\pm \delta m$ within which 68% of the results fall. Using the LB (NN) method, 6% (25%) of the simulated experiments produce a σ_m which is smaller than we obtain. For an “accurate subset” of the MC ensembles with mean σ_m/m_t that matches our value, δm is smaller.

Fits to data Quantity fit	LB fit		NN fit				
	value	σ_{stat}	value	σ_{stat}			
$m_t(\text{GeV}/c^2)$	174.0	± 5.6	171.3	± 6.0			
n_s	23.8	$^{+8.3}_{-7.8}$	28.8	$^{+8.4}_{-9.1}$			
n_b	53.2	$^{+10.7}_{-9.3}$	48.2	$^{+11.4}_{-8.7}$			
Systematic error on m_t	Energy scale		± 4.0				
	Generator		± 4.1				
	Other		± 2.2				
Resulting m_t (GeV/ c^2) 173.3 \pm 5.6(stat) \pm 6.2(syst)							
Fits to MC (top + background)	type of fit	m_t	input			output	
			$\langle n_s \rangle$	$\langle n_b \rangle$	$\langle \sigma_m \rangle$	$\langle m_t \rangle$	δm
Full ensemble	LB	175	24	53	9.9	175.0	8.7
Full ensemble	NN	172	29	48	8.5	171.6	8.0
Accurate subset	LB	175	24	53	5.5	175.3	4.6
Accurate subset	NN	172	29	48	5.8	172.0	6.0

results m_t^{LB} and m_t^{NN} are mutually consistent; in 21% of MC experiments they are further apart. Nevertheless, we include half of $m_t^{\text{LB}} - m_t^{\text{NN}}$ in the systematic error. To obtain our result, shown in Table I, we combine m_t^{LB} and m_t^{NN} allowing for their $(88 \pm 4)\%$ correlation (determined by MC experiments). Figures 3(a) and 3(b) show that this result represents the data well. From the MC experiments summarized in Table I we measure the interval $\pm \delta m$ within which 68% of the MC estimates fall. For the full ensemble, δm is larger than σ_m from our data. However, for “accurate subsets” of the ensemble for which the average σ_m/m_t is the same as we observe, δm is close to σ_m [11].

A principal systematic error in m_t arises from uncertainty in the jet energy scale, which is calibrated in three steps. In step 1, applied before events are selected, the summed energy E_{jet} of particles emitted within the jet cone is related [12] to the measured energy E_m by $E_{\text{jet}} = (E_m - O)/R(1 - S)$. Here the calorimeter response R is calibrated using $Z \rightarrow ee$ decays and E_T balance in $\gamma + \text{jet}$ events, the fractional shower leakage S out of the jet cone is set by test beam data, and the energy offset O due to noise and the underlying event is determined using events with multiple interactions. Steps 2 and 3 are applied only to jet energies used to find m_{fit} . In step 2, top MC is used to correct E_{jet} to the parton energy in both data and MC. This sharpens the resolution in m_{fit} . Step 3 is a final adjustment based on a more detailed study of $\gamma + \text{jet}$ events in data and MC, particularly focused on the dependence of the E_T balance upon η of the jet. We assign a jet-scale error of $\pm(2.5\% + 0.5 \text{ GeV})$ based on the internal consistency of step 3, on variations of the $\gamma + \text{jet}$ cuts and the model

for the underlying event, and on an independent check of the E_T balance in $Z + \text{jet}$ events. This leads to an error on m_t of $\pm 4.0 \text{ GeV}/c^2$.

We estimate the uncertainties in modeling of QCD by substituting the ISAJET MC generator [13] for HERWIG, independently for top MC and for VECBOS fragmentation, by changing the VECBOS QCD scale from jet $\langle p_T \rangle^2$ to M_W^2 , and by varying the amount of initial and final state gluon radiation in the top MC. The resulting systematic error due to the generator is $\pm 4.1 \text{ GeV}/c^2$. Other effects including noise, multiple $p\bar{p}$ interactions, and differences in fits to $\ln L$ contribute $\pm 2.2 \text{ GeV}/c^2$. All systematic errors (Table I) sum in quadrature to $\pm 6.2 \text{ GeV}/c^2$. Therefore our direct measurement of the top quark mass is $m_t = 173.3 \pm 5.6$ (stat) ± 6.2 (syst) GeV/c^2 .

We thank the staffs at Fermilab and the collaborating institutions for their contributions to this work and the Department of Energy and National Science Foundation (U.S.), Commissariat à l’Energie Atomique (France), State Committee for Science and Technology and Ministry for Atomic Energy (Russia), CNPq (Brazil), Departments of Atomic Energy and Science and Education (India), Colciencias (Colombia), CONACyT (Mexico), Ministry of Education and KOSEF (Korea), CONICET and UBACyT (Argentina), and the A. P. Sloan Foundation for support.

*Visitor from Universidad San Francisco de Quito, Quito, Ecuador.

†Visitor from IHEP, Beijing, China.

- [1] CDF Collaboration, F. Abe *et al.*, Phys. Rev. Lett. **74**, 2626 (1995); D0 Collaboration, S. Abachi *et al.*, Phys. Rev. Lett. **74**, 2632 (1995).
- [2] D0 Collaboration, S. Abachi *et al.*, Phys. Rev. D **52**, 4877 (1995); Nucl. Instrum. Methods Phys. Res., Sect. A **338**, 185 (1994).
- [3] G. Marchesini *et al.*, Comput. Phys. Commun. **67**, 465 (1992), release 5.7.
- [4] F. A. Berends *et al.*, Nucl. Phys. **B357**, 32 (1991), release 3.0.
- [5] We add cuts on \mathcal{A} and H_T to measure $\sigma(p\bar{p} \rightarrow t\bar{t})$ in the $\ell + \text{jets}$ channel. D0 Collaboration, S. Abachi *et al.*, following Letter, Phys. Rev. Lett. **79**, 1203 (1997).
- [6] S. Snyder, Ph.D. thesis, (State Univ. of New York, Stony Brook, 1995) (unpublished), http://www-d0.fnal.gov/publications_talks/thesis/snyder/thesis-ps.html
- [7] D0 Collaboration, M. Strovink *et al.*, Proceedings of the 11th Topical Workshop on $p\bar{p}$ Collider Physics, Padova, 1996 (Report No. Fermilab-Conf-96/336-E) (to be published).
- [8] E. K. Blum and L. K. Li, Neural Networks **4**, 511 (1991); D. W. Ruck *et al.*, IEEE Trans. Neural Networks **1**, 296 (1990); L. Lönnblad *et al.*, Comput. Phys. Commun. **81**, 185 (1994); D0 Collaboration, P. C. Bhat *et al.*, in *Proceedings of the 10th Topical Workshop on $p\bar{p}$ Collider Physics, Fermi National Accelerator Laboratory, 308, 1995* (Report No. Fermilab-Conf-95/211-E. We used JETNET 3.0).
- [9] P. C. Bhat, H. B. Prosper, and S. Snyder, Fermilab-Pub-96/397, Phys. Lett. B (to be published).
- [10] D0 Collaboration, S. Protopopescu *et al.*, and CDF Collaboration, J. Lys *et al.* in Proceedings of the International Conference on High Energy Physics, Warsaw, 1996 (Report No. Fermilab-Conf-97/013-E and Report No. Fermilab-Conf-96/409-E) (to be published).
- [11] We have varied our analysis procedures (e.g., the binning of D) in ways which have little systematic effect on MC results. From data we observe little change in m_t , together with variations in σ_m which are of the same order as those of δm in Table I. We interpret the variations in σ_m as stochastic effects to which the MC studies in Table I are relevant.
- [12] D0 Collaboration, R. Kehoe *et al.* in Proceedings of the 6th International Conference on Calorimetry in High Energy Physics, Frascati, 1996 (Report No. Fermilab-Conf-96/284-E) (to be published).
- [13] F. Paige and S. Protopopescu, BNL Report No. BNL38034, 1986 (unpublished), release 7.22. In many QCD studies, ISAJET is in much less acceptable agreement than HERWIG with D0 data.